Flavor and CP Violation with Fourth Generations Revisited

Wei-Shu Hou[1,2] and Chien-Yi Ma[1]
[1]Department of Physics, National Taiwan University, Taipei, Taiwan 10617
[2]National Center for Theoretical Sciences, North Branch, National Taiwan University, Taipei, Taiwan 10617
(Dated: April 22, 2010)

The Standard Model predicts a very small CP violation phase $\sin 2\Phi_{B_s}^{\rm SM} \simeq -0.04$ in B_s–$\bar{B}_s$ mixing. Any finite value of Φ_{B_s} measured at the Tevatron would imply New Physics. With recent hints for finite $\sin 2\Phi_{B_s}$, we reconsider the possibility of a 4th generation. As recent direct search bounds have become considerably heavier than 300 GeV, we take the t' mass to be near the unitarity bound of 500 GeV. Combining the measured values of Δm_{B_s} with $\mathcal{B}(B \to X_s \ell^+ \ell^-)$, together with typical f_{B_s} values, we find a sizable $\sin 2\Phi_{B_s}^{\rm SM4} \sim -0.33$. Using $m_{b'} = 480$ GeV, we extract the range $0.06 < |V_{t'b}| < 0.13$ from the constraints of $\Gamma(Z \to b\bar{b})$, Δm_D and $\mathcal{B}(K^+ \to \pi^+ \nu\bar{\nu})$. A future measurement of $\mathcal{B}(K_L \to \pi^0 \nu\bar{\nu})$ will determine $V_{t'd}$.

PACS numbers: 11.30.Er, 11.30.Hv, 12.60.Jv, 13.25.Hw

I. INTRODUCTION

There has been a recent mild revival [1] for the 4 generation Standard Model (SM4). In good measure, this is due to some hint [2] for finite CP violation (CPV) phase $\sin 2\Phi_{B_s}$ at the Tevatron, which seems to resonate with the unanticipated large deviation between direct CPV asymmetries, observed by the B factories, between charged vs neutral B meson decays to $K\pi$ final states (the so-called $\Delta A_{K\pi}$ problem [3]). The 3 generation Standard Model (SM, or SM3) predicts $\sin 2\Phi_{B_s}^{\rm SM} \equiv \arg M_{12} \simeq \arg (V_{ts}^* V_{tb})^2 \sim -\lambda^2\eta \simeq -0.04$, where λ and η are parameters of the Wolfenstein parametrization of the 3 generation CKM matrix [4]. However, by its nondecoupling behavior, the heavy t' quark is especially suited to make impact on the above $b \to s$ processes [5–7].

Another reason of the mild revival is in regards electroweak precision tests (EWPT). Some analyses show that even if the oblique parameter T is tuned to 0.232 ± 0.045 in SM4, the quality of the electroweak global fit still deteriorates considerably ($\Delta\chi^2 = 6.8$, disfavored at the 99% CL) [4]. However, the conclusion arises from the strong prejudice of keeping M_H fixed at the same SM3 value of 117 GeV. Several papers [8–10] demonstrate that, if M_H is taken as input variable, as is done for SM3, one could attain fits that are sometimes better than SM3 in some parameter space. Although this issue has recently been reopened [11], as we are concerned with the flavor and CP front, we will take the EWPT issue just at that: an open question.

A third motivation for taking the 4th generation seriously is the fundamental problem of CPV itself. While the unique CPV phase in SM3 has been verified spectacularly by the B factories, but as exemplified by the hint for $\sin 2\Phi_{B_s}$, it may be just a mirage. It is well known that the intrinsic CPV in SM3 falls short of the requirement of the second Sakharov condition by a factor of at least 10^{10}. However, as noted by one of us, if one simply extends SM3 to SM4, by being able to replace the rather light second generation quark masses with the very heavy fourth generation masses, the intrinsic CPV in SM4 may jump by 10^{15} [12] compared to SM3, and would seem sufficient for generating the matter dominance of the Universe. Although the third Sakharov condition remains an issue, this still elevates the value for the pursuit of the 4th generation. The recent successful collision of the Large Hadron Collider (LHC) at 7 TeV certainly ups the ante of the search game, be it $\sin 2\Phi_{B_s}$, or direct search for the t' and b' quarks themselves.

Refs. [6, 7] have studied flavor and CPV issues in B, K and D systems. However, $m_{t'} = 300$ GeV was used, qualified by the statement that a change in $m_{t'}$ would correspond to some change in the CKM factors, with the gross features retained. With the rising recent interest, and direct search bounds now considerably above 300 GeV [13, 14], we revisit the flavor and CPV effects of a 4th generation with a higher t' mass. Our purpose is not to make a fit, since we deem it premature, and could be misleading. Instead, we more or less follow Refs. [6] and [7], emphasizing salient features. Also, although we touch upon the still developing measurement of D^0–$\bar{D}^0$ mixing, we avoid incorporating the uncontrolled long distance or hadronic effects such as $\Delta A_{K\pi}$.

In the next section, we will discuss $\sin 2\Phi_{B_s}$ by comparing Δm_{B_s} and $\mathcal{B}(b \to s\ell\ell)$, and predict a possibly large deviation from SM3, due to heavy t' interfering with t through a nontrivial $V_{t's}^* V_{t'b}$. In Sec. III, we give an estimate of $V_{t'b}$, taking into consideration $\Gamma(Z \to b\bar{b})/\Gamma(Z \to \text{hadrons})$, $\mathcal{B}(K^+ \to \pi^+ \nu\bar{\nu})$, D^0–$\bar{D}^0$ mixing and EWPT. Taking a nominal value for $V_{t'b}$, a nominal value for $V_{t's}$ is extracted, where critical dependence would be on $m_{t'}$ and f_{B_s}. In Sec. IV, adding the constraints of ε_K and $\sin 2\Phi_{B_d}$, we discuss the correlations between $\mathcal{B}(K_L \to \pi^0 \nu\bar{\nu})$ and $\sin 2\Phi_D$, advocating the K_L measurement as more critical in determining $V_{t'd}$ in the future. We offer a brief conclusion in Sec. V.

II. LARGE $\sin 2\Phi_{B_s}$?

The measured CPV phase $\sin 2\Phi_{B_d}$ ($\equiv \sin 2\phi_1 \equiv \sin 2\beta$) via $B_d \to J/\psi K^0$ modes is consistent with SM, i.e. SM3. However, recent measurements by the CDF and DØ experiments [2] of the analogous $\sin 2\Phi_{B_s}$ ($\equiv -\sin 2\beta_s \equiv \sin \phi_s$) in tagged $B_s^0 \to J/\psi\phi$ decays seem to give a large and negative value that is $2.1\,\sigma$ away from the SM expectation of -0.04. Though not yet significant, the central value is tantalizingly close to a prediction [6] based on the 4th generation interpretation [5] of the observed B^+ vs $B^0 \to K\pi$ direct CPV difference.

With four generations, the extra CKM product $V_{t's}^* V_{t'b}$ turns the familiar $b \to s$ unitarity triangle into a quadrangle:

$$V_{us}^* V_{ub} + V_{cs}^* V_{cb} + V_{ts}^* V_{tb} + V_{t's}^* V_{t'b} = 0. \tag{1}$$

The t' quark interferes with the top in the box diagram for B_s–$\bar{B}_s$ mixing. We will use Δm_{B_s}, together with the rare decay branching fraction $\mathcal{B}(b \to s\ell\ell)$, which is dominated by the Z–penguin diagram, to constrain the range of

$$\lambda_{t'} \equiv V_{t's}^* V_{t'b} \equiv r_{sb} e^{i\phi_{sb}}, \tag{2}$$

and gain a handle [6, 7] on $\sin 2\Phi_{B_s}$. Both the box and the Z–penguin diagrams are quite susceptible to the non-decoupled t' effects [15] through $V_{t's}^* V_{t'b}$. The present study explores variations in f_{B_s} and $m_{t'}$.

Since the main source of information is from B physics, we use the convenient parametrization of Ref. [16] for the 4×4 CKM matrix, where the 4th row and 3rd column are kept particularly simple. We list the following elements for sake of later discussions:

$$V_{t'd} = -c_{24}c_{34}s_{14}e^{-i\phi_{db}}, \tag{3}$$
$$V_{t's} = -c_{34}s_{24}\,e^{-i\phi_{sb}}, \tag{4}$$
$$V_{t'b} = -s_{34}, \tag{5}$$
$$V_{t'b'} = c_{14}c_{24}c_{34}, \tag{6}$$
$$\begin{aligned} V_{ub'} = {} & c_{12}c_{13}s_{14}\,e^{i\phi_{db}} + c_{13}c_{14}s_{12}s_{24}\,e^{i\phi_{sb}} \\ & + c_{14}c_{24}s_{13}s_{34}\,e^{-i\phi_{ub}}, \end{aligned} \tag{7}$$
$$\begin{aligned} V_{cb'} = {} & c_{12}c_{14}c_{23}s_{24}\,e^{i\phi_{sb}} - c_{23}s_{12}s_{14}\,e^{i\phi_{db}} \\ & + c_{13}c_{14}c_{24}s_{23}s_{34} - c_{14}s_{12}s_{13}s_{23}s_{24}\,e^{i(\phi_{sb}+\phi_{ub})} \\ & - c_{12}s_{13}s_{14}s_{23}e^{i(\phi_{db}+\phi_{ub})}. \end{aligned} \tag{8}$$

The form of $V_{tb'}$ is also more complicated, but $V_{ub} = c_{34}s_{13}e^{-i\phi_{ub}}$, $V_{cb} = c_{13}c_{34}s_{23}$, $V_{tb} = c_{13}c_{23}c_{34}$ are simple and close to the usual SM3 parametrization [4]. In the small angle limit, this allows us to take the PDG values for s_{12}, s_{23}, s_{13}, as well as $\phi_{ub} = \phi_3 \cong 60^\circ$ as inputs, so $V_{ij} \simeq V_{ij}^{\rm SM}$ for $i = u, c$ and $j = d, s, b$. From (1), one can also express

$$\lambda_t \equiv V_{ts}^* V_{tb} \simeq -r_{sb}e^{i\phi_{sb}} - \lambda_u^{\rm SM} - \lambda_c^{\rm SM} \tag{9}$$

in terms of r_{sb} and ϕ_{sb}. The notation of ϕ_{sb}, ϕ_{db} and ϕ_{ub} follows that of Ref. [7].

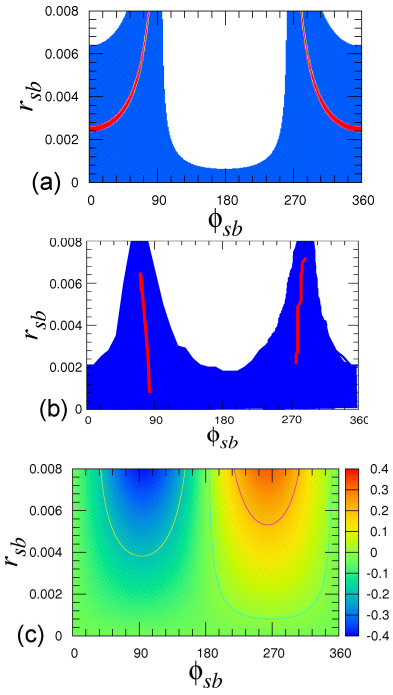

Fig. 1. The allowed blue (or dark) range in ϕ_{sb}–r_{sb} from (a) $\Delta m_{B_s}^{\rm exp}$ due mainly to the lattice uncertainty in $f_{B_s}\hat{B}_{B_s}^{1/2} = 266(18)$ MeV, and (b) $\mathcal{B}^{\rm exp}(b \to s\ell\ell) = (4.5 \pm 1.0) \times 10^{-6}$, where the red (or grey) lines correspond to taking the central values of 266 MeV and 4.5×10^{-6}, respectively. In (c), values of $\sin 2\Phi_{B_s}$ are plotted over ϕ_{sb}–r_{sb} space. All plots are for $m_{t'} = 500$ GeV.

The formula for Δm_{B_s} is well known,

$$\begin{aligned} M_{12} = {} & \frac{G_F^2 M_W^2}{12\pi^2} m_{B_s} f_{B_s}^2 \hat{B}_{B_s} \Big[\lambda_t^2 \eta S_0(x_t) \\ & + \eta' \lambda_{t'}^2 S_0(x_{t'}) + 2\tilde{\eta}\lambda_t\lambda_{t'}\tilde{S}_0(x_t, x_{t'})\Big]. \end{aligned} \tag{10}$$

Let us first consider the case of $m_{t'} = 500$ GeV. Even though $\Delta m_{B_s}^{\rm exp} = (17.77 \pm 0.12)\,{\rm ps}^{-1}$ is precisely measured, the error for the current lattice value for $f_{B_s}\hat{B}_{B_s}^{1/2}$ allows a large range for r_{sb} and ϕ_{sb}, as shown in Fig. 1(a), where we have taken a recent result of $f_{B_s}\hat{B}_{B_s}^{1/2} = 266(18)$ MeV [17] for illustration. For $b \to s\ell\ell$ decay, we follow the NNLO calculation of Ref. [18]. However, as shown in Fig. 1(b), here the experimental measurement of $\mathcal{B}^{\rm exp}(b \to s\ell\ell) = (4.5 \pm 1.0) \times 10^{-6}$ [4] has a sizable error, hence also allows a large range [19] in r_{sb}, ϕ_{sb}.

Comparing Figs. 1(a) with (b), and projecting onto the $\sin 2\Phi_{B_s}$ value plotted in Fig. 1(c), we still have a lot of range for possible $\sin 2\Phi_{B_s} \sim (-0.4, 0.0)$ values. Note that positive $\sin 2\Phi_{B_s}$, the righthand side of Fig. 1(c), is ruled out by $\Delta\mathcal{A}_{K\pi}$ [6, 7]. For illustration, let us take the central values for $f_{B_s}\hat{B}_{B_s}^{1/2}$ and $\mathcal{B}^{\rm exp}(b \to s\ell\ell)$, illustrated by the (light) red lines in Figs. 1(a) and (b). We find $\sin 2\Phi_{B_s}$, r_{sb}, $\phi_{sb} = -0.33$, 0.006, 75°, respectively. If we take the higher value of $f_{B_s}\hat{B}_{B_s}^{1/2} = 295\,{\rm MeV}$, the

$V_{t's}^* V_{t'b} \backslash \sin 2\Phi_{B_s}$	$f_{B_s}\hat{B}_{B_s}^{1/2} = 266\,\text{MeV}$	$f_{B_s}\hat{B}_{B_s}^{1/2} = 295\,\text{MeV}$
$m_{t'} = 300$ GeV	$0.015\, e^{i81^\circ} \backslash -0.37$	$0.025\, e^{i70^\circ} \backslash -0.60$
$m_{t'} = 500$ GeV	$0.006\, e^{i75^\circ} \backslash -0.33$	$0.010\, e^{i61^\circ} \backslash -0.38$

Table I. Central values for $V_{t's}^* V_{t'b}$ and $\sin 2\Phi_{B_s}$, corresponding to different $m_{t'}$ and $f_{B_s}\hat{B}_{B_s}^{1/2}$ values.

same value as in the previous study [6], we then have $\sin 2\Phi_{B_s},\ r_{sb},\ \phi_{sb} = -0.38,\ 0.010,\ 61^\circ$.

The previous study was for $m_{t'} = 300$ GeV [6, 7]. Though seemingly ruled out by the Tevatron, this mass possibility still needs to be crosschecked at the LHC. Following similar procedures for this case, we find a larger $f_{B_s}\hat{B}_{B_s}^{1/2}$ value would imply an even stronger $\sin 2\Phi_{B_s}$. Taking the central value of $\mathcal{B}^{\rm exp}(b \to s\ell\ell)$, we get $\sin 2\Phi_{B_s},\ r_{sb},\ \phi_{sb} = -0.37,\ 0.015,\ 81^\circ$ for the $f_{B_s}\hat{B}_{B_s}^{1/2} = 266$ MeV case, compared with $-0.60,\ 0.025,\ 70^\circ$ for the $f_{B_s}\hat{B}_{B_s}^{1/2} = 295$ MeV case (which roughly reproduces the result of Ref. [6]). Thus, if $-\sin 2\Phi_{B_s}$ is found to be larger than 0.5 or so, then larger $f_{B_s}\hat{B}_{B_s}^{1/2}$ values would be preferred, and t' mass would be likely closer to the current Tevatron bounds. On the other hand, the somewhat elaborate discussion here is in the interest of predicting $\sin 2\Phi_{B_s}$ when only Δm_{B_s} is known, which brings in a large uncertainty through f_{B_s}. A future precision measurement would largely bypass the f_{B_s} dependence, and, together with knowledge of $m_{t'}$ and improved measurement of $\mathcal{B}(b \to s\ell\ell)$, should allow us good information on $V_{t's}^* V_{tb}$.

We summarize our results in Table I. We note that for the 295 MeV case, the central value for r_{sb} ($\equiv |V_{t's}^* V_{tb}|$) is considerably larger than for the 266 MeV case. This is because the SM3 value for Δm_{B_s} is already much higher than the experimental value, hence one would need a larger t' effect to compensate and bring it down. Higher r_{sb}, however, will raise the lower bound of $|V_{t'b}|$, which we now turn to discuss.

III. UPPER AND LOWER BOUNDS ON $|V_{t'b}|$

An upper bound on $V_{t'b}$ comes from $R_b = \Gamma(Z \to b\bar{b})/\Gamma(Z \to \text{hadrons})$ due to the loop diagram with t'. Following Ref. [20], we find

$$|V_{tb}|^2 + 3.4|V_{t'b}|^2 < 1.14, \quad m_{t'} = 300\ \text{GeV}, \quad (11)$$
$$|V_{tb}|^2 + 9.6|V_{t'b}|^2 < 1.14, \quad m_{t'} = 500\ \text{GeV}. \quad (12)$$

Applying the relatively good approximation $|V_{tb}|^2 \simeq 1 - |V_{t'b}|^2$, we get

$$|V_{t'b}| \le 0.13\ (0.24), \qquad m_{t'} = 500\ (300)\ \text{GeV}. \quad (13)$$

These upper bounds are given in Table II. Note, of course, that these bounds do not depend on f_{B_s}.

bound on $\lvert V_{t'b}\rvert$	$f_{B_s}\hat{B}_{B_s}^{1/2} = 266$ MeV	$f_{B_s}\hat{B}_{B_s}^{1/2} = 295$ MeV
$m_{t'} = 300$ GeV	(0.12, 0.24)	(0.20, 0.24)
$m_{t'} = 500$ GeV	(0.06, 0.13)	(0.10, 0.13)

Table II. Bounds on $|V_{t'b}|$ for different $m_{t'}$ (with $m_{b'}$ taken 20 GeV lower) and $f_{B_s}\hat{B}_{B_s}^{1/2}$ values. Note that the upper bound arising from $Z \to b\bar{b}$ does not depend on $f_{B_s}\hat{B}_{B_s}^{1/2}$. The lower bounds arise from a possible tension between $\mathcal{B}(K^+ \to \pi^+\nu\bar{\nu})$ and D^0–$\bar{D}^0$ mixing. See text for discussion.

A lower bound on $|V_{t'b}|$ can arise from considering $\mathcal{B}(K^+ \to \pi^+\nu\bar{\nu})$ and D^0–$\bar{D}^0$ mixing together. For the former, we use [21],

$$\kappa_+ |V_{us}|^{-10} \left|\lambda_c^{ds}|V_{us}|^4 P_c + \lambda_t^{ds}\eta_t X_0(x_t) + \lambda_{t'}^{ds}\eta_{t'} X_0(x_{t'})\right|^2 < 3.6 \times 10^{-10}\ (90\%\ \text{CL}), \quad (14)$$

with $\lambda_q^{ds} \equiv V_{qd}V_{qs}^*$, and the 90% CL bound is from $\mathcal{B}^{\rm exp}(K^+ \to \pi^+\nu\bar{\nu}) = (1.73^{+1.15}_{-1.05}) \times 10^{-10}$ [22]. We define $V_{t'd}^* V_{t's} \equiv r_{ds} e^{i\phi_{ds}}$.

For Δm_D, where b' enters the loop, we follow the formulas and ansatz in Ref. [23, 24],

$$\begin{aligned} M_{12}^D \propto\ & \lambda_s^2 S_0(x_s) + 2\lambda_s\lambda_b S(x_s, x_b) + \lambda_b^2 S_0(x_b) + LD \\ & + 2\lambda_s\lambda_{b'} S(x_s, x_{b'}) + 2\lambda_b\lambda_{b'} S(x_b, x_{b'}) + LD \\ & + \lambda_{b'}^2 S_0(x_{b'}), \end{aligned} \quad (15)$$

where here $\lambda_q \equiv V_{uq}^* V_{cq}$. The first three terms of the first line are the short distance SM3 contributions. But experiment suggest sizable long distance (LD) contributions, since y_D is comparable [25] to x_D. Indeed, current data is consistent with D^0–$\bar{D}^0$ mixing as due entirely to LD effect. The second line involves both 4th and a lower generation appearing in the box, but even here, there could be LD effects. To allow for these two types of LD effects, we take the purely short distance $|V_{ub'}^* V_{cb'}|^2 S_0(x_{b'})$, i.e. the last term, and equate it with $x_D^{\rm exp}$, but enlarging it by a factor of 3. We then find

$$|V_{ub'}^* V_{cb'}| < (3.45^{-0.27}_{+0.35}) \times 10^{-3}, \quad (16)$$

for $m_{b'} = 260 \pm 30$ GeV, and

$$|V_{ub'}^* V_{cb'}| < (2.20^{-0.12}_{+0.13}) \times 10^{-3}, \quad (17)$$

for $m_{b'} = 460 \pm 30$ GeV, where we have applied the latest experimental value of $x_D^{\rm exp} = (9.1^{+2.5}_{-2.6}) \times 10^{-3}$ [25]. The range for $m_{b'}$ contains the sample value we would use for illustration.

With these set up, we can now discuss how a lower bound on $|V_{t'b}|$ could arise. From Eqs. (3)–(8), $V_{t'b},\ V_{t's},\ V_{t'd}$ are proportional to $s_{34},\ s_{24},\ s_{14}$, respectively, and $|V_{cb'}| \simeq |V_{t's}|$ if s_{24} is not unduly small. But it is less likely that $V_{ub'} \propto s_{14}$ would hold, since the likely larger angles s_{24} and s_{34} enter modulated only by factors of s_{12} and s_{13}, respectively, where $s_{12} \cong \lambda \simeq 0.2$ is not particularly small. So, if $|V_{t's}^* V_{t'b}|$ is held *fixed* (in the context of definite $m_{t'}$ and $\sin 2\Phi_{B_s}$), as $|V_{t'b}| \simeq s_{34}$

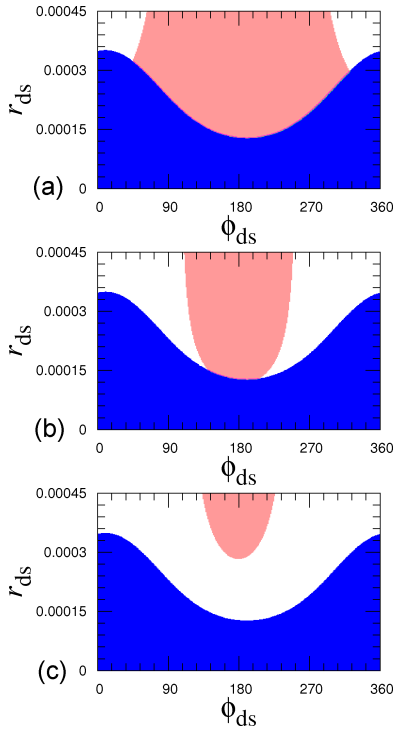

Fig. 2. Allowed regions in ϕ_{ds}-r_{ds}, where $V^*_{t'd}V_{t's} \equiv r_{ds}e^{i\phi_{ds}}$, for $\mathcal{B}(K^+ \to \pi^+\nu\bar{\nu})$ (blue or dark) and D^0–$\bar{D}^0$ mixing (pink or grey), for $m_{t'} = 500$ GeV, $m_{b'} = 480$ GeV, $V^*_{t's}V_{t'b} = 0.006\,e^{i75^\circ}$, and $|V_{t'b}|$ = (a) 0.065, (b) 0.060, (c) 0.058. For the last $|V_{t'b}|$ value, the allowed regions no longer overlap, resulting in a lower bound close to 0.06.

is lowered, $|V_{t's}| \simeq s_{24}$ would grow. To satisfy the constraint of Eq. (14), one would have to reduce $|V_{t'd}| \simeq s_{14}$. But then, from Eq. (7), $|V_{ub'}|$ would likely rise and cause tension with Eqs. (16) and (17). The form of Eq. (7), which is from the parametrization of Ref. [16], helps in elucidating this effect. With s_{14} constrained small while s_{24} looming larger, the $s_{12}s_{24}$ term would likely dominate $|V_{ub'}|$ (remember, s_{34} is pushed lower, and it is further modulated by s_{13} which is the strength of $|V_{ub}| \simeq 0.003$), while $|V_{cb'}| \simeq |V_{t's}| \simeq s_{24}$, hence the Δm_D constraint of Eq. (17) becomes hard to satisfy.

As illustrated in Fig. 2, we find that when $|V_{t'b}|$ drops below 0.06 (0.12) for $m_{t'} = 500$ (300) GeV, the regions allowed by $\mathcal{B}(K^+ \to \pi^+\nu\bar{\nu})$ and Δm_D do not intersect anymore. We conclude that, for $f_{B_s}\hat{B}^{1/2}_{B_s} = 266$ MeV,

$$|V_{t'b}| \geq 0.12, \quad (m_{t'},\, m_{b'}) = (300,\, 280)\ \text{GeV}, \quad (18)$$

for $V^*_{t's}V_{t'b} = 0.015\,e^{i81^\circ}$ (see Table I), and

$$|V_{t'b}| \geq 0.06, \quad (m_{t'},\, m_{b'}) = (500,\, 480)\ \text{GeV}, \quad (19)$$

for $V^*_{t's}V_{t'b} = 0.006\,e^{i75^\circ}$, where these are meant as points of illustration only.

For the $f_{B_s}\hat{B}^{1/2}_{B_s} = 295$ MeV case, $|V^*_{t's}V_{t'b}|$ is much larger than the 266 MeV case (Table I), which aggravates the above tension. Taking the central values for $V^*_{t's}V_{t'b}$ from Table I, we summarize the lower bounds for $|V_{t'b}|$ in Table II. Note that the 295 MeV case has a much narrower range for $|V_{t'b}|$.

nominal $V_{t'q}$	$f_{B_s}\hat{B}^{1/2}_{B_s} = 266$ MeV	$f_{B_s}\hat{B}^{1/2}_{B_s} = 295$ MeV
$m_{t'} = 300$ GeV	$V_{t'b} = -0.18$	$V_{t'b} = -0.22$
	$V_{t's} = -0.083\,e^{-i81^\circ}$	$V_{t's} = -0.1136\,e^{-i70^\circ}$
$m_{t'} = 500$ GeV	$V_{t'b} = -0.10$	$V_{t'b} = -0.12$
	$V_{t's} = -0.06\,e^{i75^\circ}$	$V_{t's} = -0.083\,e^{-i61^\circ}$

Table III. Nominal (and EWPT allowed) $V_{t'b}$ and $V_{t's}$ values for different $m_{t'}$ (with $m_{b'}$ taken 20 GeV lower) and $f_{B_s}\hat{B}^{1/2}_{B_s}$.

For illustration, we take the mean values for $|V_{t'b}|$ from Table II, combine again with the central values of $V^*_{t's}V_{t'b}$ from Table I, and give some "nominal" values for $V_{t'b}$ and $V_{t's}$, within the parametrization of the 4×4 CKM matrix of Ref. [16] in Table III. In the Appendix, we show that $|V_{t'b}|$ values near the bounds of Table II are less favored by EWPT. Furthermore, larger $|V_{t'b}|$, $|V_{t's}|$ imply larger χ^2. Thus, the lower $f_{B_s}\hat{B}^{1/2}_{B_s} \sim 266$ MeV case is probably more welcome.

IV. $K_L \to \pi^0\nu\bar{\nu}$ AND $\sin 2\Phi_D$

In Ref. [7], ε'/ε was utilized as a constraint, and non-standard hadronic parameter solutions were found for $m_{t'} \sim 300$ GeV. But as we allow $m_{t'}$ to vary, it becomes apparent that huge hadronic uncertainties preclude the utility of ε'/ε in providing a constraint. Instead, it may be more interesting to illustrate the potential impact of a future measurement of $K_L \to \pi^0\nu\bar{\nu}$, which is dominated purely by short distance. The SM predicts $\mathcal{B}^{\rm SM}(K_L \to \pi^0\nu\bar{\nu}) = (2.8 \pm 0.4) \times 10^{-11}$ [26], while the current limit is $\mathcal{B}^{\rm exp}(K_L \to \pi^0\nu\bar{\nu}) < 6.7 \times 10^{-8}$ [27]. The E14 (now KOTO) experiment, however, proposes to conduct a three-year physics run beginning in 2011, to reach of order 10 events if SM holds. Suppose 100-250 events are observed (which would be spectacular), it would imply $\mathcal{B}^{\rm exp}(K_L \to \pi^0\nu\bar{\nu}) \sim 1 \times 10^{-9}$. This value is just below the Grossman–Nir bound [28], *i.e.* $\mathcal{B}(K_L \to \pi^0\nu\bar{\nu})/\mathcal{B}(K^+ \to \pi^+\nu\bar{\nu}) \sim 4.4$, assuming that $\mathcal{B}(K^+ \to \pi^+\nu\bar{\nu})$ is itself on the higher side of the current experimental central value.

Let us take $m_{t'} = 500$ GeV and $f_{B_s}\hat{B}^{1/2}_{B_s} = 266$ MeV for illustration. We plot in Fig. 3(a) the allowed regions for $\mathcal{B}^{\rm exp}(K_L \to \pi^0\nu\bar{\nu}) \sim 1 \times 10^{-9}$ and $\varepsilon_K^{\rm exp} = (2.229 \pm 0.012) \times 10^{-3}$ [4], with $\mathcal{B}(K^+ \to \pi^+\nu\bar{\nu})$ as the broad backdrop (it can be viewed as interfaced with D^0–$\bar{D}^0$ mixing, e.g. Fig. 2(a)). Again $V^*_{t'd}V_{t's} \equiv r_{ds}e^{i\phi_{ds}}$. We find two possible solutions of $V_{t'd}$. However, one solution is ruled out by the constraint $\sin 2\Phi^{\rm exp}_{B_d} = 0.672 \pm 0.023$ [29] (see Fig. 3(c); note that with $\phi_{ub} \simeq \phi_3 \cong 60^\circ$, $\sin 2\Phi^{\rm SM}_{B_d} \simeq 0.687$ is expected), where an improvement of error by factor of 3 is also illustrated. Comparing

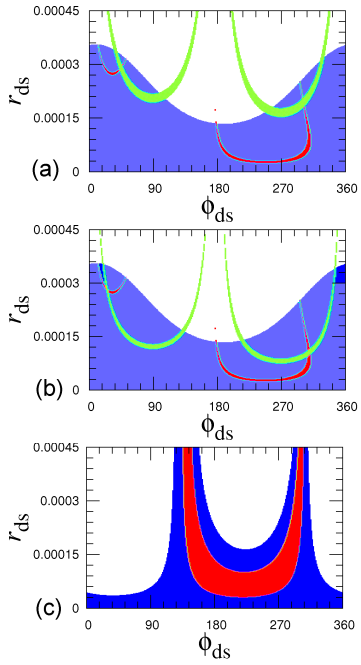

Fig. 3. Impact of future measurements of (green or light) $\mathcal{B}(K_L \to \pi^0\nu\bar{\nu}) \sim$ (a) 1×10^{-9} and (b) 3×10^{-10}, for $m_{t'} = 500$ GeV, $m_{b'} = 480$ GeV, and $V_{t'b} = -0.10$, $V_{t's} = -0.060\, e^{-i75^\circ}$, together with ε_K (red and dark grey), and combined $\mathcal{B}(K^+ \to \pi^+\nu\bar{\nu})$ and D^0–$\bar{D}^0$ mixing (blue or dark). The allowed range for $\sin 2\Phi_{B_d}^{\rm exp} = 0.672 \pm 0.023$ (blue or dark) is given in (c), together with a more precise 0.672 ± 0.008 (red or dark grey).

Fig. 3(a) and Fig. 3(c), the only possible solution is $V_{t'd} \sim -0.0032\, e^{-i18^\circ}$. *This would in fact complete the* 4×4 *CKM matrix.*

As further corollary to the full determination of the 4×4 CKM matrix, let us see how the value for $\sin 2\Phi_D$ is correlated with $K_L \to \pi^0\nu\bar{\nu}$. For this purpose, we parameterize M_{12}^D as

$$M_{12}^D = \frac{G_F^2 M_W^2}{12\pi^2}\, m_D f_D^2 B_D\, \eta(m_c, M_W) \times (\lambda_{b'}^2 + R_{LD}) S_0(x_{b'}), \qquad (20)$$

and for simplicity, we assume R_{LD} to be real (this may not be a very good assumption because the second type of LD effect in Eq. (15) could involve $\lambda_{b'}$ linearly). This allows, by varying within $m_{b'} = 460 \pm 30$ GeV, to find $\sin 2\Phi_D \simeq 0.13$, and $|\cos 2\Phi_D| \simeq 0.99$, which are consistent with current data [29]. These values can serve as a corollary for consistency check in the future. But it should be clear that one would need to find a better handle on LD effects.

To illustrate a smaller value for $\mathcal{B}^{\rm exp}(K_L \to \pi^0\nu\bar{\nu})$, we take the value of 3×10^{-10} (still 10 times the SM value) and replot in Fig. 3(b). Compared with 3(a), it can be noted that the two branches for $\mathcal{B}^{\rm exp}(K_L \to \pi^0\nu\bar{\nu})$ are less symmetric and each less parabolic. This is simply because for Fig. 3(a), the 4th generation effect is pre-

Real R_{LD}	
$\mathcal{B}_{K_L\to\pi^0\nu\bar{\nu}} = 9.2\times10^{-10}$	$V_{t'd} = -0.0032\, e^{-i18^\circ}$
$\varepsilon_K = 2.229\times10^{-3}$	$\mathcal{B}_{K^+\to\pi^+\nu\bar{\nu}} = 2.1\times10^{-10}$
$x_D = 9.1\times10^{-3}$	
$m_{t'} = 500$ GeV	$\lvert\lambda_{b'}^2 + R_{LD}\rvert = (16.2^{-1.6}_{+1.9})\times10^{-7}$
$m_{b'} = 460 \pm 30$ GeV	$\lambda_{b'}^2 = (8.0 + 2.1i)\times10^{-7}$
$V_{t'b} = -0.10$	$\sin 2\Phi_D \simeq 0.13$
$V_{t's} = -0.06\, e^{-i75^\circ}$	$\lvert\cos 2\Phi_D\rvert \simeq 0.99$

Table IV. A scenario for future measurement of large $\mathcal{B}(K_L \to \pi^0\nu\bar{\nu})$, where $\lambda_{b'} = V_{ub'}^* V_{cb'}$. Taking R_{LD} as real, we can get $\sin 2\Phi_D$ and $\cos 2\Phi_D$ once a full 4×4 CKM matrix is determined, where we illustrate with a finite range for $m_{b'}$. The left-hand side are inputs.

dominant, hence the allowed lowest r_{ds} value is for ϕ_{ds} purely imaginary. For the lower $\mathcal{B}^{\rm exp}(K_L \to \pi^0\nu\bar{\nu})$ case of Fig. 3(b), the top effect matters more, causing some qualitative change. In any case, for the intersection of the allowed regions of $\mathcal{B}^{\rm exp}(K_L \to \pi^0\nu\bar{\nu}) \sim 3\times10^{-10}$ and ε_K in Fig. 3(b), we find $V_{t'd} \sim -0.0018\, e^{-i22^\circ}$, and a much smaller imaginary part for $\lambda_{b'} = V_{ub'}^* V_{cb'}$, hence $\sin 2\Phi_D$ would drop considerably. This can be understood by noting that $V_{ub'}$ is now dominated by the second term in Eq. (7), i.e. $|s_{14}/s_{12}s_{24}| \sim 0.14$, while $V_{cb'}$ is always dominated by the first s_{24} term in Eq. (8), hence the large associated phase of ϕ_{sb} largely cancels. The long distance R_{LD} effect would only further dilute $\sin 2\Phi_D$. Therefore, we do not quote any value for $\sin 2\Phi_D$, except that, if $\mathcal{B}^{\rm exp}(K_L \to \pi^0\nu\bar{\nu})$ is on the low side, then one should expect $\sin 2\Phi_D$ to be rather small as well. Note that, as can be seen from Fig. 3(c), if the central value for $\sin 2\Phi_{B_d}$ remains, but with error reduced by a factor of 3, tension would arise. Thus, future $\sin 2\Phi_{B_d}$ measurement would provide a crosscheck.

We summarize the more spectacular scenario of $\mathcal{B}^{\rm exp}(K_L \to \pi^0\nu\bar{\nu}) \sim 1\times10^{-9}$, which nearly saturates the Grossman–Nir bound, in Table IV. The more specific values given in this Table are recalculated from the intersection values for ϕ_{ds} and r_{ds}. We also give the approximate values of the 4×4 CKM matrix,

$$\begin{bmatrix} 0.974 & 0.225 & 0.0036e^{-i60^\circ} & 0.015\, e^{i64^\circ} \\ -0.226 & 0.972 & 0.041 & 0.060\, e^{i72^\circ} \\ 0.008\, e^{-i22^\circ} & -0.043e^{-i7^\circ} & 0.994 & 0.099e^{-i1^\circ} \\ -0.003e^{-i18^\circ} & -0.06e^{-i75^\circ} & -0.1 & 0.993 \end{bmatrix}$$

which we do not aim at any precision, just to illustrate the $m_{t'} = 500$ GeV case, and compare with the numerical values given 5 years ago in Ref. [7] for the $m_{t'} = 300$ GeV case. As discussed, this is for an optimal value for $\mathcal{B}(K_L \to \pi^0\nu\bar{\nu})$ for the future measurement at the KOTO experiment. If the measured value for $\mathcal{B}(K_L \to \pi^0\nu\bar{\nu})$ is lower, then the strength and phase of $V_{t'd}$ would further drop, the details depending also on the intersection with ε_K as well as the precise $m_{t'}$ value. But the $V_{ub'}$ value would be less affected. Note also that $\mathcal{B}(K^+ \to \pi^+\nu\bar{\nu}) = 2.1\times10^{-10}$ is a little on the high

side compared to current measurement, but not by too much. Of course, if measurement of $\sin 2\Phi_D$ could get ahead of $\mathcal{B}^{\rm exp}(K_L \to \pi^0\nu\bar\nu)$, information of $V_{t'd}$ can also be extracted. But it would depend on our understanding of the LD effects, which appears difficult. From our discussion, we also see that a larger $\sin 2\Phi_D$ value would likely imply a large $\mathcal{B}(K_L \to \pi^0\nu\bar\nu)$.

V. DISCUSSION AND CONCLUSION

A 4th generation is a very natural extension of the Standard Model, as we already have 3 generations. It is curious why the famed measurement of $\sin 2\Phi_{B_d}$ at the B factories came out consistent with SM3, while there is also the tension in EWPT measurements. However, with the LHC finally starting, we are entering an era where the question of whether there is a 4th generation can be answered once and for all [30] by direct search. This paper surveys the flavor and CPV aspects, focusing on where information may be extracted. For this reason, we have not used the experimentally established $\Delta A_{K\pi}$, nor ε'/ε, as these are marred by long-distance or hadronic effects. We did use the Δm_D measurement. Although LD effects also enters, the measured strength still puts a constraint on the combination of $|V^*_{ub'}V_{cb'}|m^2_{b'}$.

We illustrated with a series of steps on how a full 4×4 CKM matrix can be determined, from the present towards the future. We took mainly $m_{t'} = 500$ GeV, $m_{b'} = 480$ GeV and $f_{B_s}\hat B^{1/2}_{B_s} = 266$ MeV as an example. First, combining the constraints of Δm_{B_s} and $\mathcal{B}(b \to s\ell\ell)$, where the nondecoupling nature of the t' quark could make its effect felt, one could determine $V^*_{t's}V_{t'b} \sim 0.006\, e^{i75^\circ}$. This leads to a predicted range for $\sin 2\Phi_{B_s}$, the measurement of which is of great current interest at the Tevatron and LHC. In turn, once $\sin 2\Phi_{B_s}$ is measured with suitable precision, it would provide us with a probe of $V^*_{t's}V_{t'b}$, although Δm_{B_s} would still be marred by f_{B_s}, and we would still rely on measurements such as $\mathcal{B}(b \to s\ell\ell)$. Second, R_b gives rise to an upper bound of $|V_{t'b}| < 0.13$, and from combining $\mathcal{B}(K^+ \to \pi^+\nu\bar\nu)$ and D^0–$\bar D^0$ mixing, one could extract a lower bound of $|V_{t'b}| > 0.06$. This follows from the assumption that $|V^*_{t's}V_{t'b}|$ is known. Then, a lower $|V_{t'b}|$ means a higher $|V_{t's}|$. The bound from $\mathcal{B}(K^+ \to \pi^+\nu\bar\nu)$ then demands a smaller $|V_{t'd}|$, which in turn limits the ability for $|V_{ub'}|$ to satisfy the Δm_D constraint. In the Appendix, we show that the bounds on $|V_{t'b}|$ is consistent with EWPT constraints, but the central value is (and generally, smaller $|V_{t'b}|$ and $|V_{t's}|$ values are) preferred. For sake of illustration, we offer $V_{t'b} = -0.10$ and $V_{t's} = -0.06\, e^{-i75^\circ}$ (in the parametrization of Ref. [16]) as nominal values for $m_{t'}$, $m_{b'} = 500$, 480 GeV.

There is insufficient information at present to pin down $V_{t'd}$, but this can be achieved with a future measurement of $K_L \to \pi^0\nu\bar\nu$. Suppose $\mathcal{B}(K_L \to \pi^0\nu\bar\nu) = 10^{-9}$ is found by the KOTO experiment. With the current data on $\mathcal{B}(K^+ \to \pi^+\nu\bar\nu)$, this is close to saturating the Grossman–Nir bound, so it is probably optimistic. By combining with ε_K as a constraint, we get two possible solutions of $V_{t'd}$. Then, taking into account the constraint of $\sin 2\Phi_{B_d}$ (the measurement of which should also improve), this selects out the solution $V_{t'd} = -0.0032\, e^{-i18^\circ}$ (again in the parametrization of Ref. [16]). So, it seems that within a decade, we may determine the complete 4×4 CKM matrix.

For the time being, with LHC experiments soon to catch up with the vigorous pursuit of the measurement of $\sin 2\Phi_{B_s}$ and direct t', b' search at the Tevatron, if we consider the uncertainties from $f_{B_s}\hat B^{1/2}_{B_s}$ and $\mathcal{B}(b \to s\ell\ell)$, $\sin 2\Phi_{B_s}$ can range from -0.4 to 0. As the t' mass bound rises, one expects a weaker, but still negative, $\sin 2\Phi_{B_s}$. We see that the critical future measurement beyond $\sin 2\Phi_{B_s}$ would be $\mathcal{B}(K_L \to \pi^0\nu\bar\nu)$, which is also purely short distance, and can help us determine $V_{t'd}$. The measurement of $\sin 2\Phi_{B_d}$ by all means should also be improved. The usage of CPV in D mixing, $\sin 2\Phi_D$, would require knowledge of long distance effects.

Note Added. While writing this paper, similar discussions have also been made by Soni *et al.* [31] and Buras *et al.* [32], with differences in emphasis than our approach.

Acknowledgement. The work of WSH is supported in part by NSC97-2112-M-002-004-MY3 and NTU-98R0066. The work of CYM is supported by NSC98-2811-M-002-103.

APPENDIX

In a recent paper by Chanowitz [10], the 4th generation corrections to the oblique parameters S, T were considered, which enter

$$M_W^2 = \left(M_W^{\rm SM}\right)^2 \left[1 - \frac{\alpha\Delta S}{2(c_w^2 - s_w^2)} + \frac{c_w^2\alpha\Delta T}{(c_w^2 - s_w^2)}\right], \quad (21)$$

$$\sin^2\theta^{\rm lept}_{\rm eff} = \sin^2\theta^{\rm lept}_{\rm eff}|^{\rm SM} \left[1 + \frac{\alpha\Delta S}{4s_w^2(c_w^2 - s_w^2)} - \frac{c_w^2\alpha\Delta T}{(c_w^2 - s_w^2)}\right], \quad (22)$$

and

$$\Gamma(Z \to \nu\bar\nu) = \Gamma^{\rm SM}(Z \to \nu\bar\nu)\,[1 + \alpha\Delta T]\,. \quad (23)$$

These formulas can be found in Ref. [33]. Here, we neglect all other parameters U, V, W, X, Y, but we extend formulas $\sin^2\theta^{\rm lept}_{\rm eff}$ to $\sin^2\theta^f_{\rm eff}$ and $\Gamma(Z \to \nu\bar\nu)$ to $\Gamma(Z \to f\bar f)$. Though it is not our main concern, following Chanowitz, we also wish to investigate the impact of considering quark mixing on the electroweak observables.

Compared to S, T, which come from vacuum polarization corrections, one also has to include the vertex corrections from Fig. 4 (touched upon in Sec. III for upper bound on $V_{t'b}$; note that the vacuum polarization effects largely cancel in the ratio of R_b), which cause the shift

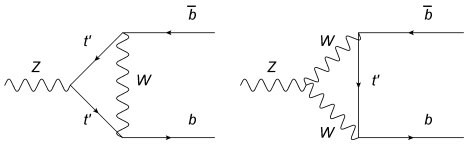

Fig. 4. One-loop correction to $Zb\bar{b}$ vertex from t'.

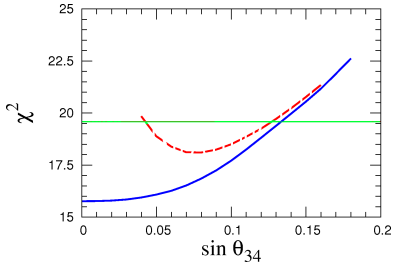

Fig. 5. For $m_{t'} = 500$ GeV, $m_{b'} = 480$ GeV, $m_{\ell_4} = 145$ GeV, $m_{\nu_4} = 100$ GeV: solid (blue) χ^2 vs $|V_{t'b}| = s_{34}$ for $s_{24} = s_{14} = 0$; and dashed (red) χ^2 vs s_{34} for $V^*_{t's}V_{t'b} = 0.006\, e^{i75^\circ}$.

to $Zb\bar{b}$ couplings

$$v_b = v_b^{\rm SM} + \delta g_{bL}, \tag{24}$$

$$a_b = a_b^{\rm SM} + \delta g_{bL}, \tag{25}$$

where $v_b^{\rm SM} = -\frac{1}{2} + \frac{2}{3}s_w^2$, $a_b^{\rm SM} = -\frac{1}{2}$, and δg_{bL} is given in Ref. [10]. Hence, the effective couplings g_V^b, g_A^b become

$$g_V^b = \sqrt{\rho_Z^b}\left(-\frac{1}{2} + \frac{2}{3}\sin^2\theta_{\rm eff}^b\right)\frac{v_b}{v_b^{\rm SM}} \tag{26}$$

$$g_A^b = \sqrt{\rho_Z^b}\left(-\frac{1}{2}\right)\frac{a_b}{a_b^{\rm SM}}. \tag{27}$$

Inserting this into the formula [34] for $\Gamma(Z \to q\bar{q})$ is

$$\Gamma(Z \to q\bar{q}) = \frac{\alpha\, M_Z}{4 s_w^2 c_w^2}\left(|a_q^{\rm SM}|^2 + |v_q^{\rm SM}|^2\right)\left(1 + \delta_q^{(0)}\right)\cdots,$$

we then have the complete correction formula

$$\Gamma(Z \to b\bar{b}) = \Gamma^{\rm SM}(Z \to b\bar{b})\,[1 + \alpha\Delta T]\,\frac{|a_b|^2 + |v_b|^2}{|a_b^{\rm SM}|^2 + |v_b^{\rm SM}|^2}. \tag{28}$$

We then follow the procedures given in Ref. [10]. Neglecting Γ_W fit and including the correlation matrices in Ref. [35], we use ZFITTER 6.4.2 to successfully reproduce the results of Ref. [10]. With this attained, we take $m_{t'} = 500$ GeV, $m_{b'} = 480$ GeV, $m_{\ell_4} = 145$ GeV, $m_{\nu_4} = 100$ GeV, and set $s_{14} = s_{24} = 0$, The plot of χ^2 vs s_{34} is given in Fig. 5 as the solid (blue) curve. The best fit occurs at $s_{34} = 0$ with $\chi^2_{\rm min} = 15.8$, and 95% CL is located at $\chi^2 = 19.6$.

Next, we consider the case of taking $V^*_{t's}V_{t'b} = 0.006\, e^{i75^\circ}$ (see Table I), as motivated by our flavor and CPV analysis. We see from the dashed (red) curve in Fig. 5 that 95% CL is located at $s_{34} = 0.04$ and 0.13, with the lowest χ^2 at $s_{34} = 0.08$ (the lower s_{34} value would could trouble through a rather large $V_{t's}$). The rise in χ^2 away from $s_{34} = 0.08$ is in part due to fixing $|V^*_{t's}V_{t'b}|$ at 0.006. But with this treated as external to the fit, the change in χ^2 is not much worse than treating the effect of $V_{t'b}$ in the loop but ignoring $V_{t's}$. Note that the latter affects $Z \to s\bar{s}$, but this process is hard to separate experimentally.

[1] B. Holdom, W.-S. Hou, T. Hurth, M.L. Mangano, S. Sultansoy and G. Ünel, PMC Phys. A **3**, 4 (2009).

[2] See http://tevbwg.fnal.gov/results/Summer2009_betas/; and as reported by G. Punzi at Europhysics Conference on High Energy Physics, Krakow, Poland, July, 2009 [arXiv:1001.4886 [hep-ex]].

[3] S.-W. Lin, Y. Unno, W.-S. Hou, P. Chang *et al.* [Belle collaboration], Nature **452**, 332 (2008).

[4] C. Amsler *et al.* [Particle Data Group], Phys. Lett. B **667**, 1 (2008).

[5] W.-S. Hou, M. Nagashima and A. Soddu, Phys. Rev. Lett. **95**, 141601 (2005); W.-S. Hou, H.-n. Li, S. Mishima and M. Nagashima, *ibid.* **98**, 131801 (2007).

[6] W.-S. Hou, M. Nagashima, A. Soddu, Phys. Rev. D **76**, 016004 (2007).

[7] W.-S. Hou, M. Nagashima, A. Soddu, Phys. Rev. D **72**, 115007 (2005).

[8] H.-J. He, N. Polonsky and S.-f. Su, Phys. Rev. D **64**, 053004 (2001).

[9] G.D. Kribs, T. Plehn, M.S. Spannowsky and T.M.P. Tait, Phys. Rev. D **76**, 075016 (2007).

[10] M. Chanowitz, Phys. Rev. D **79**, 113008 (2009).

[11] J. Erler and P. Langacker, arXiv:1003.3211 [hep-ph].

[12] W.-S. Hou, Chin. J. Phys. **47**, 134 (2009) [arXiv:0803.1234 [hep-ph]].

[13] T. Aaltonen *et al.* [CDF Collaboration], Phys. Rev. Lett. **100**, 161803 (2008). Updates available on CDF webpage http://www-cdf.fnal.gov/.

[14] T. Aaltonen *et al.* [CDF Collaboration], Phys. Rev. Lett. **104**, 091801 (2010).

[15] W.-S. Hou, R.S. Willey and A. Soni, Phys. Rev. Lett. **58**, 1608 (1987) [Erratum-ibid. **60**, 2337 (1988)].

[16] W.-S. Hou, A. Soni and H. Steger, Phys. Lett. B **192**, 441 (1987).

[17] E. Gamiz *et al.* [HPQCD Collaboration], Phys. Rev. D **80**, 014503 (2009).

[18] C. Bobeth, M. Misiak and J. Urban, Nucl. Phys. B **574**, 291 (2000). Beware of a few typos (cf. arXiv:hep-ph/9910220).

[19] One could use the measurement of foward-backward asymmetry in $B \to K^*\ell\ell$, especially the large $q^2 \equiv m^2_{\ell\ell}$ part, to further constrain the 4th generation parame-

ters; see C. Bobeth, G. Hiller, and G. Piranishvili, JHEP **0807**, 106 (2008). This would be an interesting direction to pursue in the future, when the lower q^2 discrepancy is better established and understood. For this aspect, see also A. Hovhannisyan, W.-S. Hou and N. Mahajan, Phys. Rev. D **77**, 014016 (2008).

[20] T. Yanir, JHEP**0206**, 044 (2002).

[21] A.J. Buras, F. Schwab and S. Uhlig, Rev. Mod. Phys. **80** 965 (2008).

[22] V.A. Artamonov *et al.* [E949 Collaboration], Phys. Rev. Lett. **101**, 191802 (2008).

[23] M. Bobrowski, A. Lenz, J. Riedl and J. Rohrwild, Phys. Rev. D **79**, 113006 (2009).

[24] Besides considerations in Refs. [7] and [6], a standard earlier reference is E. Golowich, J. Hewett, S. Pakvasa, A.A. Petrov, Phys. Rev. D **76**, 095009 (2007).

[25] E. Barberio *et al.* [Heavy Flavor Averaging Group (HFAG)], arXiv:0808.1297 [hep-ex].

[26] F. Mescia, C. Smith, Phys. Rev. D **76**, 034017 (2007).

[27] J. Ahn *et al.* [E391a Collaboration], Phys. Rev. Lett. **100**, 201802 (2008);

[28] Y. Grossman and Y. Nir, Phys. Lett. B **398**, 163 (1997).

[29] E. Barberio *et al.* [Heavy Flavor Averaging Group (HFAG)], arXiv:0704.3575 [hep-ex].

[30] A. Arhrib and W.-S. Hou, JHEP **0607**, 009 (2006).

[31] A. Soni, A.K. Alok, A. Giri, R. Mohanta and S. Nandi, arXiv:1002.0595 [hep-ph].

[32] A.J. Buras, B. Duling, T. Feldmann, T. Heidsieck, C. Promberger and S. Recksiegel, arXiv:1002.2126 [hep-ph].

[33] I. Maksymyk, C.P. Burgess and D. London, Phys. Rev. D **50**, 529 (1994).

[34] J. Bernabéu, A. Pich and A. Santamaria, Nucl. Phys. **363**, 326 (1991).

[35] The ALEPH, DELPHI, L3, OPAL and SLD Collaborations, the LEP Electroweak Working Group, and the SLD Electroweak and Heavy Flavour Groups, Phys. Rept. **427**, 257 (2006).